



ELSEVIER

Biophysical Chemistry 88 (2000) 47–59

Biophysical  
Chemistry

www.elsevier.nl/locate/bpc

# Designing drugs to stop the formation of prion aggregates and other amyloids

Joanna Masel<sup>a,\*</sup>, Vincent A.A. Jansen<sup>a,b</sup>

<sup>a</sup>Wellcome Trust Centre for the Epidemiology of Infectious Disease, Department of Zoology, University of Oxford, South Parks Road, Oxford, OX1 3PS, UK

<sup>b</sup>School of Biological Sciences, Royal Holloway, University of London, Egham, Surrey TW20 0EX, UK

Received 19 June 2000; accepted 25 July 2000

## Abstract

Amyloid protein aggregates are implicated in many neurodegenerative diseases, including Alzheimer's disease and the prion diseases. Therapeutics to block amyloid formation are often tested in vitro, but it is not clear how to extrapolate from these experiments to a clinical setting, where the effective drug dose may be much lower. Here we address this question using a theoretical kinetic model to calculate the growth rate of protein aggregates as a function of the dose of each of three categories of drug. We find that therapeutics which block the growing ends of amyloids are the most promising, as alternative strategies may be ineffective or even accelerate amyloid formation at low drug concentrations. Our mathematical model can be used to identify and optimise an end-blocking drug in vitro. Our model also suggests an alternative explanation for data previously thought to prove the existence of an entity known as protein X. © 2000 Elsevier Science B.V. All rights reserved.

*Keywords:* Prion disease; Replication mechanism; Alzheimer's disease; Amyloid formation; Therapeutics; Mathematical model

## 1. Introduction

An infectious form of the PrP protein (PrP<sup>Sc</sup>) causes transmissible spongiform encephalopathies such as scrapie and Creutzfeldt–Jakob disease by converting the normal form of PrP (PrP<sup>C</sup>) into PrP<sup>Sc</sup>, according to the widely accepted prion

theory [1]. Purified prion preparations contain aggregated PrP in the conformationally altered form of amyloid, and this amyloid or its precursors may be the infectious agent [2]. Abnormal protein aggregates, including amyloids, have also been implicated in the pathogenesis of other neurodegenerative diseases such as Alzheimer's disease, Huntington's disease and Parkinson's disease.

Drugs which block amyloidogenesis are now being identified, often using in vitro assays. It is not clear which of these candidate drugs are most

\* Corresponding author. Present address: Department of Biological Sciences, Stanford University, Stanford, CA 94305, USA.

*E-mail address:* joanna.masel@zoo.ox.ac.uk (J. Masel).

likely to be safe and effective in a clinical setting, where conditions may be very different from those in vitro. In particular, the effective drug dose may be very low in vivo. Here we use mathematical models to address this question by expressing the rate of amyloid accumulation as a function of drug dose. These models help to extrapolate from in vitro results to predict behaviour at the low drug doses which more closely resemble in vivo conditions. Our models are grounded in basic mechanistic principles of polymer kinetics, and so they can be applied to any macroscopically linear polymers, whether amyloid fibrils, protofibrils or some other protein aggregate. The term ‘macroscopically linear abnormal protein aggregate’ is cumbersome, so in this paper we use the word amyloid, but our results should be taken to apply more generally.

To formulate a suitable mathematical model, we need a reasonable idea of the kinetic mechanism of amyloid formation and propagation. For most amyloid diseases, the nucleated polymerisation mechanism is well-accepted [3]. For the prion diseases, there is considerable controversy over which of the rival nucleated polymerisation and template-assistance hypotheses is a better description of prion kinetics [4,5]. Most discussions of their relative merits have focused on the kinetics of the de novo formation of prions [5,6]. Since sporadic prion diseases occur at a very low incidence of approximately  $10^{-6}$ , we can assume that the rate of de novo prion formation is negligible in vivo. In this paper we focus on seeded or template-assisted formation, which is clearly the most relevant process in infectious disease. The two rival hypotheses do not differ greatly on the kinetic mechanism of seed or template-assisted replication, and may under some formulations be kinetically equivalent, as shown in Fig. 1. Our results apply equally under the nucleated polymerisation and template-assistance hypotheses, and so the words template, seed and nucleus should be considered interchangeable in this manuscript.

Because the infectiousness of prion diseases makes more in vivo data available, we first consider the prion replication mechanism. For prions

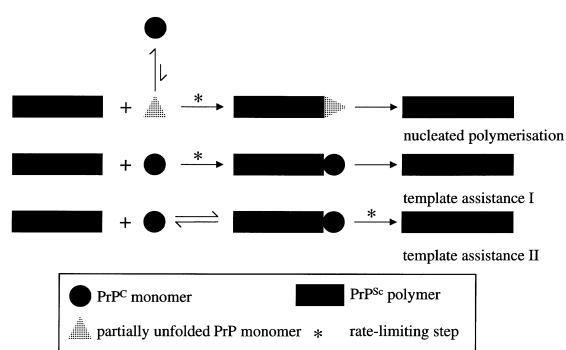


Fig. 1. Kinetics of polymer elongation. According to the nucleated polymerisation hypothesis, prions interact with a partially unfolded form of the PrP monomer (triangle), which is in rapid equilibrium with the normal form (circle). According to the template assistance hypothesis, prions interact directly with the normal PrP monomer. Under nucleated polymerisation and one possible formulation of template assistance, the rate-limiting step in polymer elongation is the interaction of a polymer and either the partially unfolded or the normal PrP monomer. Under the second formulation of template assistance, the polymer end acts as a form of catalyst, and conformational change rather than binding may be rate-limiting.

to replicate, PrP<sup>C</sup> must bind to the PrP<sup>Sc</sup> template and be converted via a conformational change to PrP<sup>Sc</sup>. If this were the only process, then all prion growth would be a result of the elongation of pre-existing seeds by the addition of more PrP<sup>Sc</sup> subunits to form ever-longer fibrils or polymers. A single seed would not be able to initiate disease, making it difficult to explain infectious prion disease.

A full kinetic description of the system should also include the rate at which new seeds are formed. In inherited disease or in in vitro studies, it is possible that new seeds are continuously formed de novo. For infectious prion diseases however, prion polymers must either catalyse the formation of new polymers along their surface, a process known as heterogeneous nucleation [7], or must break along their length to form two shorter polymers. A polymer cannot grow indefinitely, so some level of breakage seems likely. Kinetic models which ignore both breakage and heterogeneous nucleation and consider only de novo formation and polymer elongation [2,8–10],

predict that amyloid accumulation is slower than exponential [4]. This is not in agreement with data showing that prion amyloid accumulates exponentially in the brain [11,12]. Exponential growth as a result of disassociation or breakage into two replication-competent seeds or templates is postulated under both the nucleated polymerisation hypothesis [4,13], and under the template-assistance hypothesis [5,13]. Exponential growth explains why PrP amyloid is normally detectable only in the very late stages of the incubation period, when exceptionally large clusters of amyloid polymers become visible as amyloid plaques.

The exponential growth rate is clearly the most relevant parameter for the replication of infectious prions. This exponential growth rate is dependent on the kinetics of the entire system of polymers of diverse lengths, incorporating both polymer elongation and polymer breakage. Polymer elongation involves at least two steps, namely PrP<sup>C</sup> binding to the PrP<sup>Sc</sup> catalyst or template, and PrP<sup>C</sup> conversion via a conformational change to PrP<sup>Sc</sup>. The difference between template assistance and nucleated polymerisation centres on whether conformational change is rate-limiting [6]. A rate-limiting step is normally defined in the context of a series of sequential reactions. It is not clear what a 'rate-limiting' step means in the context of a replication cycle where the products of one reaction eventually feed back to become the substrates of the same reaction. The question of whether conformational change is rate-limiting can be posed for the process of polymer elongation, as shown in Fig. 1, but its meaning is not clear for the overall kinetics of the system of elongation and breakage.

New seeds may be formed either by heterogeneous nucleation or by breakage, and the two systems have very different kinetics [14]. Kinetic models of heterogeneous nucleation predict exponential growth at a rate which is highly dependent on the monomer concentration [15]. Prion incubation periods have only a mild dependence on the PrP gene dosage [16], ruling out heterogeneous nucleation. A low kinetic dependence on monomer concentration is also seen for yeast prions in vitro [17]. In contrast, an excellent quantitative fit to the PrP data was found using a

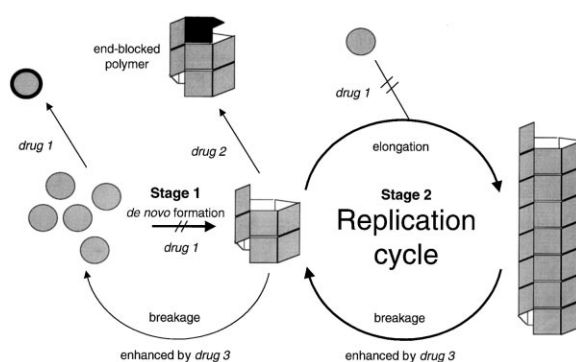


Fig. 2. Three ways to inhibit amyloidogenesis. After nuclei form or are introduced by infection, amyloid accumulates through a cycle of polymer elongation and polymer breakage. Drug 1 lowers the effective monomer concentration. This can occur via inhibiting monomer production, trafficking or processing, or by binding to and stabilising a non-pathogenic monomer or oligomer. Lowering the monomer concentration inhibits de novo formation, and slows polymer elongation. Drug 2 is similar enough to occupy a site in the ordered polymer, but different enough to disrupt the regular structure. This is analogous to poisoning the formation of a regular crystal [34]. In the context of macroscopically linear polymers, this is equivalent to blocking or capping the ends of the polymers [26]. Drug 3 fragments polymers. Moderate levels of breakage are necessary for rapid replication, but very high levels will progressively break down polymers until only monomers are left.

kinetic model of polymer elongation and breakage in which conformational change was not rate-limiting, and de novo formation was ignored [18]. In this paper, we extend previous work on this kinetic model [18,19].

In summary, prion amyloid grows from seeds which either form de novo or are introduced by infection. A general scheme of amyloid accumulation is shown in Fig. 2. We can divide amyloid accumulation into two kinetic stages. In the first kinetic stage, new templates are formed de novo, followed by polymer elongation. In the second kinetic stage, most new amyloid seeds or templates are formed by breakage, as part of a replication cycle of polymer elongation and breakage. De novo seed formation representing the first stage occurs at a constant rate until the monomer is depleted, while the rate of seed formation by breakage increases over time in proportion to the amount of accumulated amyloid. The first kinetic

stage may therefore be a good description of early events in amyloidogenesis in inherited disease or in *in vitro* studies, while the second kinetic stage becomes a better description later in the process of amyloidogenesis.

There is no hard evidence about the time course of the accumulation of other amyloids, such as that of amyloid beta peptide (A $\beta$ ) amyloid during Alzheimer's disease. It is possible that the first kinetic stage is a sufficient description of the pathogenesis of non-transmissible diseases. We argue, however, that some level of polymer breakage seems likely, and that the exponential nature of amyloid accumulation is likely to be similar for both PrP and many other amyloids. In support of this, seeding of A $\beta$  amyloid can be seen *in vivo* under some conditions [20,21].

Drugs that prevent *de novo* formation may work as a prophylactic, but may not help if *de novo* formation has already occurred and amyloid is already accumulating exponentially according to the second kinetic stage. Once amyloid replication is seeded by infectious introduction of nuclei, as seems to be the case with transmissible prion diseases, then therapeutics that prevent *de novo* formation will have no effect. Generally, preventing or merely slowing amyloid propagation seems more promising than preventing *de novo* formation. We will concentrate on therapeutics that do exactly this, by calculating how the exponential accumulation rate of the second kinetic stage varies with the dose of different categories of therapeutics.

## 2. Comparing therapeutic mechanisms

As shown in Fig. 2, amyloid accumulation can be inhibited: (1) by lowering the effective monomer concentration; (2) by blocking growing polymer ends; or (3) by increasing the polymer breakage rate. To investigate which strategy is most likely to be safe and effective in a clinical setting, we extended a mathematical model of the second kinetic stage of amyloid replication [18,19], as described in Appendix A.

Our mathematical model of the second kinetic stage can be described in general terms as follows

and as shown in Fig. 3. We consider both the case when conformational change is rate-limiting for polymer elongation, and the case when it is not, as shown in Fig. 1. Polymers require a minimum number of subunits for the infectious conformation to be stable, greater than one but perhaps quite small, but there is no arbitrary maximum polymer size. Normal and end-blocking monomers are produced and degraded. Without the infectious introduction of polymers, both would be in homeostasis. Polymers may grow from either end, but can be capped at only one end. When a polymer is introduced, one of four things may happen. It may be degraded, it may grow by incorporating a new monomer at its end, it may break at any point along its length, or its end may be capped by an end-blocking drug. Once a polymer has been capped, it may either be degraded, break at any point along its length, dissociate from the cap, or grow from the uncapped end. This system leads to exponential growth, at a rate given by Eq. (6) when conformational change is not rate-limiting, and by one of Eqs. (7)–(10) more generally. We derive Eqs. (6)–(10) in Appendix A, taking into account all the processes mentioned above.

At high doses, a breakage drug may destroy amyloid *in vitro*, and thus seem a good drug candidate. At low doses, however, a breakage drug may accelerate fibrillogenesis by providing a larger number of ends to serve as sites for replication [22]. We can see mathematically that the accumulation rates in Eqs. (6) and (7) are maximal at an intermediate level of breakage  $b$  [18]. Any drug that breaks amyloids into pieces therefore seems a dangerous drug to try on humans, especially since small oligomers have been shown to be more neurotoxic [23]. This danger of varying the dose is not merely academic: Congo red, for example has been shown to accelerate amyloid formation at low doses and to slow amyloid formation at high doses, both in a deposition assay [24], and in cell culture [25]. Eqs. (6)–(10) all show that end-blocking and monomer lowering drugs are 'safe' in that fibrillogenesis inhibition always increases with increasing drug dosage.

Monomer-lowering drugs reduce the exponential growth rate through their effect on the poly-

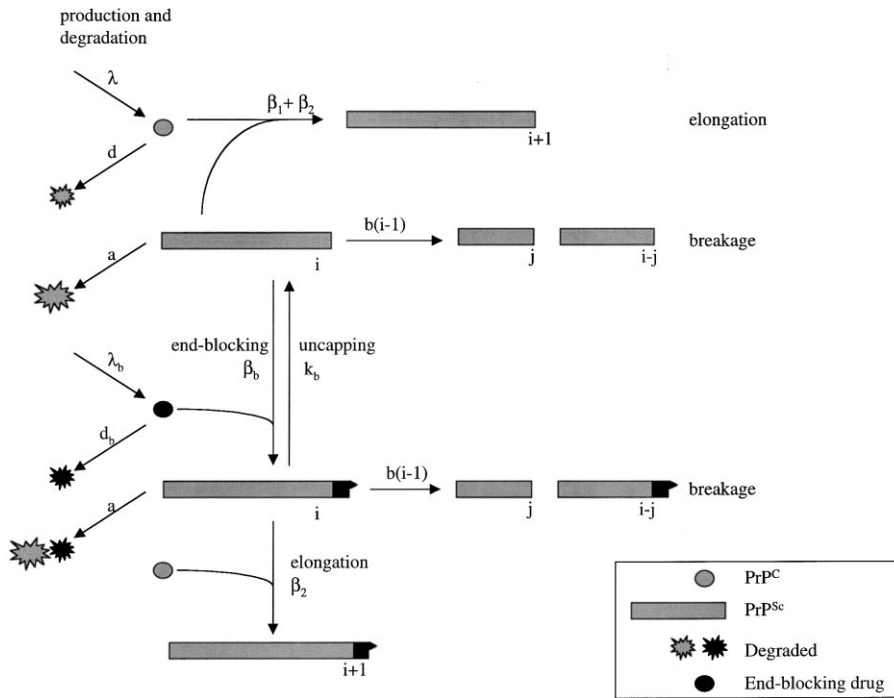


Fig. 3. Kinetic scheme of prion replication in the presence of an end-blocking drug. In this diagram, conformational change is not rate-limiting, but the process of polymer elongation may in fact take any of the three forms shown in Fig. 1. On the left, production and degradation of monomers and the end-blocking drug are shown. An uncapped polymer can either grow, break, be blocked, or be degraded. A capped polymer can either break or be degraded. In this scheme,  $i$  and  $j$  refer to polymer lengths and all other symbols refer to the rate constants.

mer elongation rate. We show in Eq. (6) that the amyloid growth rate depends only on approximately the square root of the monomer concentration when conformational change is not rate-limiting. When conformational change becomes rate-limiting, there is even less dependence on the monomer concentration, as shown in Eq. (7). This means that monomer-lowering drugs may need very high drug doses in order to be effective, which might have the side effect of inhibiting the normal function of the monomer.

In contrast, it has been suggested that low concentrations of end-blocking drugs may be sufficient [26]. Eqs. (6) and (8)–(10) show that the extent of inhibition by an end-blocking drug is highly dependent not just on the effective drug dose, but also on the breakage rate. End-blocking drugs are less effective at high breakage rates when end-blocking fails to keep up with the num-

bers of new ends appearing. If breakage varies within the brain, compartments with fairly high breakage rates will grow the fastest [18]. These fast-growing compartments with high breakage rates could well be the most relevant to pathogenesis, while compartments with low breakage rates and very long polymers may be virtually by-products of pathogenesis. A high breakage rate represents a worst-case scenario for the effectiveness of an end-blocking drug. In Fig. 4, we look at the growth rate as a function of the end-blocking drug dosage under these worst-case conditions of high breakage and fast growth, and we see that a low dose of end-blocking drug is still sufficient to inhibit amyloid accumulation. We consider a ‘low dose’ in this context to be one in which end-blocking events are much rarer than polymer elongation events. Even lower doses of an end-blocking drug than those shown in Fig. 4

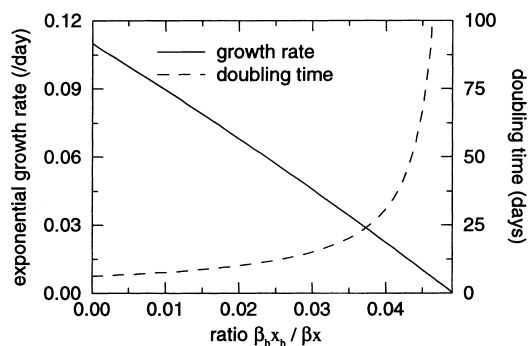


Fig. 4. Dose response curve for an end-blocking drug in vivo. The dose of end-blocking drug is expressed as a dimensionless ratio of the rate of end-blocking divided by the rate of polymer elongation. The prion doubling time and growth rate are shown as a function of the effective drug concentration. In the absence of drug, the exponential growth rate is 0.11, the minimum nucleation size  $n = 6$ , and the basic reproductive ratio is 1.5. The mean polymer size is  $3n - 1.5$ , corresponding to the high breakage rates responsible for maximal growth. Conformational change is not rate-limiting in this example, which is plotted according to Eq. (6). These parameters are plausible for prion replication in vivo [18].

would be sufficient at a lower breakage rate. We therefore conclude that an end-blocking drug is more likely to be safe and effective in a clinical setting than the other two categories of drug considered.

### 3. Designing an end-blocking drug

An effective end-blocking drug might be very similar to the amyloid protein, so that it binds to polymer ends in the same way, and yet with some subtle difference which prevents further polymer elongation [27]. An altered form of the amyloid protein itself should be ideal for these purposes. Heterologous PrP<sup>C</sup> can interfere with the in vitro conversion of homologous PrP<sup>C</sup> [28], lending support to this concept.

In vivo data also suggest that variant PrP can be an effective end-blocking drug. An elegant study on transgenic mice showed that mouse PrP<sup>C</sup> (MoPrP<sup>C</sup>) inhibits the conversion of human PrP<sup>C</sup> (HuPrP<sup>C</sup>) into HuPrP<sup>Sc</sup> in vivo [29]. MoPrP<sup>C</sup> is very similar to HuPrP<sup>C</sup> albeit with important

differences, conforming to our proposed design of an effective end-blocking drug. These data were originally explained by the hypothesis that an additional mouse protein, designated protein X, is important for conversion. Mouse protein X is hypothesised to bind MoPrP<sup>C</sup> with greater affinity than it binds HuPrP<sup>C</sup>, and so MoPrP<sup>C</sup> restricts the availability of protein X, inhibiting human prion propagation in mice.

The possibility that MoPrP<sup>C</sup> might have a direct effect on human prion propagation was rejected on the grounds that MoPrP<sup>C</sup> was present at only 10–20% of the level of HuPrP<sup>C</sup> in the brains of the transgenic mice [29]. Since heterologous MoPrP<sup>C</sup> is likely to have a lower affinity than homologous HuPrP<sup>C</sup> for HuPrP<sup>Sc</sup>, it was thought unlikely that such a low level of mouse MoPrP<sup>C</sup> would be sufficient to effectively inhibit replication through direct interaction with HuPrP<sup>Sc</sup>. At the time of this study, this seemed even more unlikely within the context of the heterodimer hypothesis of the prion replication mechanism [30], which at that time had not yet been shown to be implausible [4]. We have shown in this paper, however, that a very low effective dose of an end-blocking drug can have a large effect on replication, as illustrated in Fig. 4. This invalidates the original objection to the hypothesis that MoPrP<sup>C</sup> inhibits replication through direct interaction with HuPrP<sup>Sc</sup>. Without further evidence, both the protein X and end-blocking hypotheses can explain the transgenic mouse data, and both should be considered.

Detailed mutagenesis studies on heterologous inhibition in scrapie-infected neuroblastoma (ScN2a) cells [31,32] can in general be interpreted either as defining the protein X binding site, or as defining the optimal sequence for effective end-blocking. PrP with a single point mutation can completely inhibit heterologous PrP<sup>Sc</sup> formation in ScN2a cells [31,33]. This inhibition was diminished in PrP mutants containing more than one point mutation, relative to PrP containing any one of the point mutations [33]. This result is in perfect agreement with our proposed design of an end-blocking drug, which should be only subtly different from the replicating PrP. In contrast,

working under the protein X hypothesis, this result was considered ‘unexpected’ [33].

Peptides may make more effective end-blocking drugs than full-length proteins, since they are better able to cross the blood–brain barrier, and the possible effectiveness of peptides is supported by data. The [URE3] prion, composed of aggregated Ure2p, can be cured by fragments of Ure2p [34]. Synthetic PrP peptides can inhibit PrP conversion [35], and modified PrP peptides cause partial reversion of PrP<sup>Sc</sup> to its normal state [36]. Peptides and modified peptides inhibit A $\beta$  fibrillogenesis [37–39]. The injection of synthetic human A $\beta$ <sub>42</sub> can inhibit the formation of A $\beta$  amyloid in the PDAPP mouse model of Alzheimer’s disease [40]. This inhibition was originally hypothesised to be due to an immune response to the injected peptide, but the possibility that synthetic A $\beta$ <sub>42</sub> has sufficient subtle differences to endogenous A $\beta$  to directly inhibit amyloid formation also needs to be considered, especially since A $\beta$ <sub>42</sub> could well have crossed the blood–brain barrier [41]. The immune-based hypothesis could be distinguished experimentally from the end-blocking peptide hypothesis by looking for amyloid inhibition in SCID mice. Until this experiment is carried out, both hypotheses can explain the data, and both should be considered.

#### 4. Identifying, characterising and optimising end-blocking drugs

A $\beta$  can be rapidly assembled into amyloid in vitro. Many drugs, including peptides, inhibit this aggregation, but how can we use this assay to confirm whether a given drug works via the end-blocking mechanism? This task is simplest if the in vitro assay can be modelled by the second kinetic stage. This can be ascertained from the shape of the sigmoidal growth curve [14,42]. If the assay is dominated by the first kinetic stage, then amyloid accumulation can be detected almost immediately. If the assay is dominated by the second stage, then a very marked lag phase can be seen during which time no amyloid is visible.

Three distinct quantities can be measured using the A $\beta$  in vitro assay: the lag time until

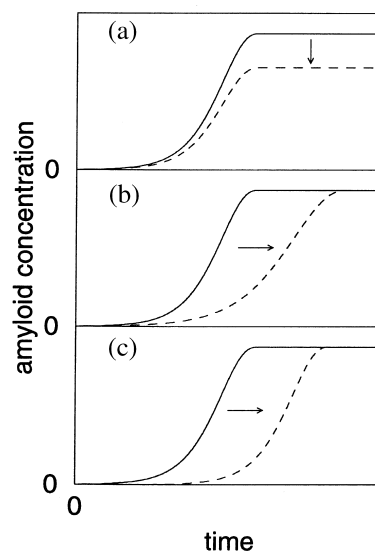


Fig. 5. Schematic diagrams of the time course of amyloid formation in the presence and absence of a drug, illustrating three different ways that the inhibition of amyloidogenesis can be observed. A real drug may of course combine more than one of the three effects. (a) The final extent of fibrillogenesis is reduced, but the time taken to reach maximum amyloid concentration is unchanged. This indicates a thermodynamic rather than a kinetic inhibitor. (b) The exponential accumulation rate is decreased, increasing the lag time until fibril formation. The two curves cannot be superimposed. The final extent of fibrillogenesis is unchanged. This indicates a kinetic rather than a thermodynamic inhibitor. (c) De novo formation is delayed, increasing the lag time by a different mechanism. The two curves can be superimposed. Again, the final extent of fibrillogenesis is unchanged.

fibrillogenesis in the presence of the drug (kinetic inhibition); the final concentration of fibrils in the presence of the drug (thermodynamic inhibition); and the disassembly rate of pre-existing fibrils [38,43]. The first two quantities are illustrated in Fig. 5.

The measurement of lag time may vary between laboratories. It is sometimes taken as the time between the start of the reaction and the point at which fibrils can first be detected. This method is obviously dependent on the sensitivity of the detection method, which is a serious disadvantage. Alternatively, a straight line is sometimes fitted through the sigmoidal data at the point of inflection, and is extrapolated back to zero product to

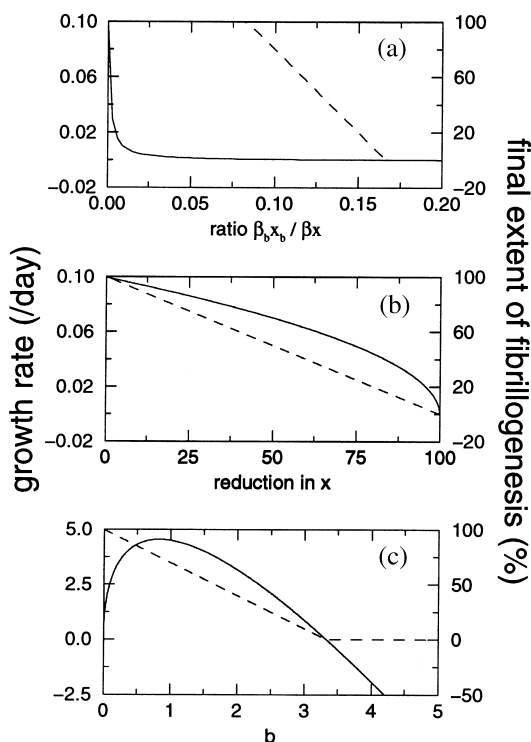


Fig. 6. The growth rate (solid line) and final extent of fibrillogenesis (dashed line) are shown as a function of drug dose in vitro. The final extent of fibrillogenesis is calculated as the equilibrium state  $\dot{z}$  in Eq. (5) with parameters:  $\lambda = 0$ ;  $\lambda_b = 0$ ;  $d = 0$ ;  $d_b = 0$ ;  $a = 0$ ;  $k_b = 0$ ;  $n = 6$ ;  $x(0) = 100$ ;  $x_b(0) = 1$ ;  $\beta_1 = 1$ ;  $\beta_2 = 0$ ;  $\beta_b = 1$ ; and  $b = 0.0001$ . Conformational change is not rate-limiting. Parameters are different to in vivo parameters in Fig. 4. In particular, breakage is likely to be slow in vitro. (a) End-blocking drug. The dose is expressed as a dimensionless ratio of the rate of end-blocking divided by the rate of polymer elongation. (b) Monomer lowering drug. The dose represents the extent of the reduction either in the monomer concentration  $x$  or more generally in the polymer elongation rate  $(\beta_1 + \beta_2)x$ . (c) Breakage drug. The dose represents the breakage rate  $b$ .

calculate the lag time. This method is more consistent, but relies on having high quality data. Another method involves measuring the time needed to generate a certain proportion of the final product such as one half or one tenth. However it is measured, the lag time of an unseeded reaction will include contributions from de novo formation. The lag time of a seeded reaction can be used to calculate the exponential growth rate

of the second kinetic stage alone, ruling out all de novo formation effects. For this to work, the initial quantity of seed must be many orders of magnitude less than the final quantity of fibrils formed. One way of achieving this might be by seeding a reaction with the last remnants of a dissociation reaction [44]. Once the growth rate is measured, we can distinguish between drug mechanisms by examining how the growth rate and final extent of fibrillogenesis vary with drug dosage in vitro, as shown in Fig. 6.

The disassembly rate of pre-existing fibrils is obviously important if therapeutics are to be effective in reversing rather than merely arresting the later stages of disease. If polymer elongation is completely blocked by an end-blocking or monomer-lowering drug, then the continuing process of breakage should lead to the gradual disappearance of polymers. This has been observed experimentally in a conditional model of Huntington's disease, where switching off the expression of mutant huntingtin does not merely halt, but actually reverses the course of the disease [45]. In vitro, much lower levels of breakage may occur, and so disassembly will be very slow, especially if the sample is not rotated or stirred. Partial reversal has, however, been seen using PrP peptides in vitro [36]. In contrast, breakage drugs should lead to rapid disassembly.

For further analysis, a very different kinetic assay can be used to measure the deposition rate of radiolabelled A $\beta$  peptides in the absence of de novo formation or breakage [24]. This can be modelled using Eq. (5) as a perturbation of equilibrium by the addition of monomer  $x$  and/or end-blocking drug  $x_b$  with breakage rate  $b = 0$ .

Low doses of end-blocking drugs will only be sufficient if binding is highly specific to the fibril ends. When binding can be measured separately from fibrillogenesis, the amount of drug bound should be proportional to the number of polymers, rather than to the amount of polymerised protein. Sonication should increase the number of binding sites for an end-blocking drug. For polymers at equilibrium, the number of polymers, and thus the number of binding sites, should be proportional to the square root of the amount of polymerised protein [46]. This relationship is

observed for labelled PrP in in vitro conversion experiments [46,47]. IDOX was found to bind with high affinity to one site for every 415 molecules of insulin amyloid, but it was not ascertained whether the number of sites remained constant after sonication or other manipulations [48]. This in vitro analysis can be used to compare variants of a known end-blocking drug in order to optimise its specificity and effectiveness.

### Acknowledgements

We thank Bob May, Elizabeth Coulson, Hester Korthals Altes and Oliver Monti for helpful discussions. JM gratefully acknowledges the support of the Rhodes Trust and VAAJ of The Wellcome Trust (Grant Number 051319).

### Appendix A: Mathematical model

Assume for now that polymers can grow from both ends, but are capped only at one end. This kinetic scheme is illustrated in Fig. 3. Let  $x$  be the abundance of monomers and  $x_b$  be the abundance of free end-blocking drug or cap. Let  $y_i$  be the abundance of polymers containing  $i$  subunits, and let  $y_{b,i}$  be the abundance of polymers containing  $i$  subunits, plus a cap on one end. The total abundance of uncapped polymers summed over all sizes is  $y = \sum y_i$ , and the abundance of capped polymers is  $y_b = \sum y_{b,i}$ . The total abundance of subunits incorporated into polymers is  $z = \sum iy_i + \sum iy_{b,i}$ . Monomers and caps are produced at rates  $\lambda$  and  $\lambda_b$ , and are degraded at rates  $d$  and  $d_b$ . Polymers are degraded at rate  $a$ . A polymer of size  $i$  breaks at rate  $b$  at each of the  $i - 1$  joins along its length. Polymers below a critical size  $n$  are unstable and disintegrate rapidly into monomers, i.e. polymers  $y_i$  and  $y_{b,i}$  with  $i < n$  formed by the breakage of larger polymers convert instantaneously into monomers.

The rate of polymer elongation will be limited by the number concentration of polymers  $y$ , which will initially be very low. Assume for now that conformational change is not rate-limiting. The rate-determining step is instead the frequency of

encounters between the polymers and the partially unfolded monomers (under the nucleated polymerisation hypothesis) or PrP<sup>C</sup> monomers (under the template-assistance hypothesis), as shown in Fig. 1. In this case, monomers are added to uncapped ends one and two at rates  $\beta_1 xy$  and  $\beta_2 x(y + y_b)$  respectively. Caps are added to end one at rate  $\beta_b x_b y$ . Caps dissociate from the ends of polymers at rate  $k_b$ . The addition of monomers to the ends of polymers was considered irreversible. This assumption is justified when the monomer concentration is substantially larger than the critical concentration. If dissociation of monomers is considered, the equations will not, unfortunately, close by summation.

The change in the free monomer concentration is given by the monomer production rate, less the monomer degradation rate, less the polymer elongation rate, plus a term representing the release of monomers following breakage near a polymer end, so we have

$$\frac{dx}{dt} = \lambda - dx - (\beta_1 + \beta_2)xy - \beta_2 xy_b + 2b \sum_{i=1}^{n-1} \sum_{j=i+1}^{\infty} i(y_j + y_{b,j}) \quad (1)$$

The change in the free cap concentration is given by the cap production rate, less the cap degradation rate, less the capping rate, plus the cap dissociation rate, plus a term representing the release of caps following breakage near a capped polymer end, so we have

$$\frac{dx_b}{dt} = \lambda_b - d_b x_b - \beta_b x_b y + k_b y_b + b \sum_{i=1}^{n-1} \sum_{j=i+1}^{\infty} y_{b,j} \quad (2)$$

The change in the concentration of uncapped polymers of length  $i$  is given by the elongation rate of uncapped polymers of length  $i - 1$ , less the elongation rate of uncapped polymers of length  $i$ , less the capping rate of polymers of length  $i$ , plus the cap dissociation rate from polymers of length  $i$ , less the degradation rate of

uncapped polymers of length  $i$ , less the breakage rate of uncapped polymers of length  $i$ , plus the breakage rate of larger polymers to form uncapped polymers of length  $i$ , so we have

$$\begin{aligned} \frac{dy_i}{dt} &= (\beta_1 + \beta_2)x(y_{i-1} - y_i) - \beta_b x_b y_i \\ &\quad + k_b y_{b,i} - ay_i - b(i-1)y_i \\ &\quad + b \sum_{j=i+1}^{\infty} (2y_j + y_{b,j}) \quad \text{for } i \geq n \\ y_i &= 0 \quad \text{for } i < n \end{aligned} \quad (3)$$

The change in the concentration of capped polymers of length  $i$  is given by the capping rate of polymers of length  $i$ , plus the elongation rate of capped polymers of length  $i-1$ , less the elongation rate of capped polymers of length  $i$ , less the cap dissociation rate, less the degradation rate of capped polymers of length  $i$ , less the breakage rate of capped polymers of length  $i$ , plus the breakage rate of larger capped polymers to form capped polymers of length  $i$ , so we have

$$\begin{aligned} \frac{dy_{b,i}}{dt} &= \beta_b x_b y_i + \beta_2 x (y_{b,i-1} - y_{b,i}) \\ &\quad - k_b y_{b,i} - ay_{b,i} - b(i-1)y_{b,i} \\ &\quad + b \sum_{j=i+1}^{\infty} y_{b,j} \quad \text{for } i \geq n \\ y_{b,i} &= 0 \quad \text{for } i < n \end{aligned} \quad (4)$$

Eqs. (1)–(4) can be closed by summation to give

$$\begin{aligned} \dot{x} &= \lambda - dx - (\beta_1 + \beta_2)xy - \beta_2 xy_b \\ &\quad + bn(n-1)(y + y_b) \\ \dot{x}_b &= \lambda_b - d_b x_b - \beta_b x_b y + k_b y_b + b(n-1)y_b \\ \dot{y} &= -\beta_b x_b y + k_b y_b - ay + bz \\ &\quad - (2n-1)by - bny_b \\ \dot{y}_b &= \beta_b x_b y - k_b y_b - ay_b - b(n-1)y_b \\ \dot{z} &= (\beta_1 + \beta_2)xy + \beta_2 xy_b - az - bn(n-1)(y + y_b) \end{aligned} \quad (5)$$

Assume that  $x$  and  $x_b$  are initially in a steady state. The system of  $y$ ,  $y_b$  and  $z$  is now linear, and will either accumulate or decay exponentially at the same rate according to the dominant eigenvalue of the Jacobian matrix until  $x$  or  $x_b$  become limiting. The dominant eigenvalue, and hence the exponential growth rate  $r$ , was solved using Maple V, and when  $k_b = 0$  and  $\beta_2 = 0$ , it is given by

$$\begin{aligned} r &= -a - b(n-1) - \frac{\beta_b x_b + b}{2} \\ &\quad + \sqrt{\left(\frac{\beta_b x_b + b}{2}\right)^2 + \beta_1 x b} \end{aligned} \quad (6)$$

The dose of an end-blocking drug is represented by the parameter  $x_b$ , the dose of a monomer lowering drug is represented as a decrease in the monomer concentration  $x$  or the polymer elongation rate  $\beta_1 x$  and the dose of a breakage drug is represented as an increase in the breakage rate  $b$ .

If the conditions  $k_b = 0$  or  $\beta_2 = 0$  are relaxed, then the expression for the eigenvalue is no longer very transparent. Some insight can be gained by considering the case when conformational change is rate-limiting for polymer elongation, following the second formulation of template assistance shown in Fig. 1, and keeping the conditions  $k_b = 0$  and  $\beta_2 = 0$ . In this case, we can treat the polymer end as an enzyme obeying the Michaelis–Menten equation [49]. Let  $k_+$  and  $k_-$  be the association and dissociation rates of unconverted monomers at the ends of the polymers, and let  $\gamma$  be the rate of conformational conversion. Following the Briggs–Haldane treatment, we assume that the proportion of polymers with unconverted monomers at the polymer ends reaches a steady state. Then in the absence of end-blocking, polymer elongation occurs at rate  $\gamma k_+ xy / (k_+ x + k_- + \gamma)$ , and exponential growth has the rate

$$r = -a - b\left(n - \frac{1}{2}\right) + \sqrt{\frac{b^2}{4} + \frac{\gamma x b}{x + \alpha}}$$

where

$$\alpha = \frac{k_- + \gamma}{k_+} \quad (7)$$

The degree to which conformational change is rate-limiting is given by the ratio  $\alpha/x$ . If this ratio is large, then conformational change is not rate-limiting, and Eq. (6) can be used with  $\beta_1 = \gamma/\alpha$ . If the ratio  $\alpha/x$  is very small, then conformational change is completely rate-limiting, and the exponential growth rate is independent of the monomer concentration. This case is not in agreement with in vivo data on the dependence of incubation period on the PrP gene dosage. Some intermediate level of monomer dependence is possible when  $\alpha/x$  is approximately 1. In these cases the monomer dependence is reduced, and so the monomer lowering drug strategy is even less likely to work at low drug concentrations.

There are three possibilities for the action of the end-blocking drug. If the cap binds at the same rate to polymers both with and without unconverted monomers at the end, then we can make a simple substitution into Eq. (6) to obtain the equation

$$r = -a - b(n-1) - \frac{\beta_b x_b + b}{2} + \sqrt{\left(\frac{\beta_b x_b + b}{2}\right)^2 + \frac{\gamma x b}{x + \alpha}} \quad (8)$$

This is equivalent to Eq. (6) with  $\beta_1 = \gamma/(x + \alpha)$ . If the cap will only bind to polymer ends that do not have an unconverted monomer bound, i.e. competitive inhibition, then we can derive the exponential growth rate

$$r = -a - bn - \frac{1}{2} \left( \frac{\beta_b x_b k_-}{k_+ (x + \alpha)} - b \right) + \sqrt{\frac{1}{4} \left( \frac{\beta_b x_b k_-}{k_+ (x + \alpha)} - b \right)^2 + \frac{\gamma x b}{x + \alpha}} \quad (9)$$

Similarly, if the cap will only bind to polymer

ends that have an unconverted monomer bound, then we get the exponential growth rate

$$r = -a - bn - \frac{1}{2} \left( \frac{\beta_b x_b x}{x + \alpha} - b \right) + \sqrt{\frac{1}{4} \left( \frac{\beta_b x_b x}{x + \alpha} - b \right)^2 + \frac{\gamma x b}{x + \alpha}} \quad (10)$$

When conformational change is partly rate-limiting, the effectiveness of the end-blocking drug strategy will depend on the particular drug mechanism. A specific end-blocking drug can be characterised in vitro by varying both the end-blocking drug concentration and the monomer concentration, and by comparing the results with predictions made by Eqs. (6)–(10).

## References

- [1] S.B. Prusiner, Prions, Proc. Natl. Acad. Sci. USA 95 (1998) 13363–13383.
- [2] J.T. Jarrett, P.T. Lansbury, Seeding ‘one-dimensional crystallization’ of amyloid: a pathogenic mechanism in Alzheimer’s disease and scrapie? Cell 73 (1993) 1055–1058.
- [3] J.D. Harper, P.T. Lansbury, Models of amyloid seeding in Alzheimer’s disease and scrapie: mechanistic truths and physiological consequences of the time-dependent solubility of amyloid proteins, Annu. Rev. Biochem. 66 (1997) 385–407.
- [4] M. Eigen, Prionics or the kinetic basis of prion diseases, Biophys. Chem., A 1-A 63 (1996) A1–A18.
- [5] F.E. Cohen, S.B. Prusiner, Pathologic conformations of prion proteins, Annu. Rev. Biochem. 67 (1998) 793–819.
- [6] I.V. Baskakov, C. Aagaard, I. Mehlhorn et al., Self-assembly of recombinant prion protein of 106 residues, Biochemistry 39 (2000) 2792–2804.
- [7] L.E. Orgel, Prion replication and secondary nucleation, Chem. Biol. 3 (1996) 413–414.
- [8] F. Oosawa, M. Kasai, A theory of linear and helical aggregations of macromolecules, J. Mol. Biol. 4 (1962) 10–21.
- [9] J. Hofrichter, P.D. Ross, W.A. Eaton, Kinetics and mechanism of deoxyhemoglobin S gelation: a new approach to understanding sickle cell disease, Proc. Natl. Acad. Sci. USA 71 (1974) 4864–4868.
- [10] A. Lomakin, D.B. Teplow, D.A. Kirschner, G.B. Benedek, Kinetic theory of fibrillogenesis of amyloid  $\beta$ -protein, Proc. Natl. Acad. Sci. USA 94 (1997) 7942–7947.
- [11] D.C. Bolton, R.D. Rudelli, J.R. Currie, P.E. Bendheim, Copurification of sp33-37 and scrapie agent from ham-

- ster brain prior to detectable histopathology and clinical disease, *J. Gen. Virol.* 72 (1991) 2905–2913.
- [12] K. Jendroska, F.P. Heinzel, M. Torchia et al., Proteinase-resistant prion protein accumulation in syrian-hamster brain correlates with regional pathology and scrapie infectivity, *Neurology* 41 (1991) 1482–1490.
- [13] P. Bamborough, H. Wille, G.C. Telling, F. Yehiely, S.B. Prusiner, F.E. Cohen, Prion protein structure and scrapie replication: theoretical, spectroscopic, and genetic investigations, *Cold Spring Harbor Symp. Quant. Biol.* 61 (1996) 495–509.
- [14] F. Ferrone, Analysis of protein aggregation kinetics, *Methods Enzymol.* 309 (1999) 256–274.
- [15] F.A. Ferrone, J. Hofrichter, W.A. Eaton, Kinetics of sickle hemoglobin polymerization II. A double nucleation mechanism, *J. Mol. Biol.* 183 (1985) 611–631.
- [16] S.B. Prusiner, M. Scott, D. Foster et al., Transgenic studies implicate interactions between homologous PrP isoforms in scrapie prion replication, *Cell* 63 (1990) 673–686.
- [17] A.H. DePace, A. Santoso, P. Hillner, J.S. Weissman, A critical role for amino-terminal glutamine/asparagine repeats in the formation and propagation of a yeast prion, *Cell* 93 (1998) 1241–1252.
- [18] J. Masel, V.A.A. Jansen, M.A. Nowak, Quantifying the kinetic parameters of prion replication, *Biophys. Chem.* 77 (1999) 139–152.
- [19] M.A. Nowak, D.C. Krakauer, A. Klug, R.M. May, Prion infection dynamics, *Integrative Biol.* 1 (1998) 3–15.
- [20] H.F. Baker, R.M. Ridley, L.W. Duchon, T.J. Crow, C.J. Bruton, Induction of  $\beta$ (A4)-amyloid in primates by injection of Alzheimer's-disease brain homogenate — comparison with transmission of spongiform encephalopathy, *Mol. Neurobiol.* 8 (1994) 25–39.
- [21] M.D. Kane, W.J. Lipinski, M.J. Callahan et al., Evidence for seeding of beta-amyloid by intracerebral infusion of Alzheimer brain extracts in beta-amyloid precursor protein-transgenic mice, *J. Neurosci.* 20 (2000) 3606–3611.
- [22] V.V. Kushnirov, M.D. Ter-Avanesyan, Structure and replication of yeast prions, *Cell* 94 (1998) 13–16.
- [23] M.P. Lambert, A.K. Barlow, B.A. Chromy et al., Diffusible, nonfibrillar ligands derived from A $\beta$ 1–42 are potent central nervous system neurotoxins, *Proc. Natl. Acad. Sci. USA* 95 (1998) 6448–6453.
- [24] W.P. Esler, E.R. Stimson, J.R. Ghilardi et al., A $\beta$  deposition inhibitor screen using synthetic amyloid, *Nat. Biotechnol.* 15 (1997) 258–263.
- [25] H. Rudyk, S. Vasiljevic, R.M. Hennion, C.R. Birkett, J. Hope, I.H. Gilbert, Screening Congo Red and its analogues for their ability to prevent the formation of PrP-res in scrapie-infected cells, *J. Gen. Virol.* 81 (2000) 1155–1164.
- [26] Y. Kusumoto, A. Lomakin, D.B. Teplow, G.B. Benedek, Temperature dependence of amyloid  $\beta$ -protein fibrilization, *Proc. Natl. Acad. Sci. USA* 95 (1998) 12277–12282.
- [27] J. Ghanta, C.L. Shen, L.L. Kiessling, R.M. Murphy, A strategy for designing inhibitors of  $\beta$ -amyloid toxicity, *J. Biol. Chem.* 271 (1996) 29525–29528.
- [28] M. Horiuchi, S.A. Priola, J. Chabry, B. Caughey, Interactions between heterologous forms of prion protein: binding, inhibition of conversion, and species barriers, *Proc. Natl. Acad. Sci. USA* 97 (2000) 5836–5841.
- [29] G.C. Telling, M. Scott, J. Mastrianni et al., Prion propagation in mice expressing human and chimeric PrP transgenes implicates the interaction of cellular PrP with another protein, *Cell* 83 (1995) 79–90.
- [30] F.E. Cohen, K.M. Pan, Z. Huang, M. Baldwin, R.J. Fletterick, S.B. Prusiner, Structural clues to prion replication, *Science* 264 (1994) 530–531.
- [31] S.A. Priola, B. Caughey, R.E. Race, B. Chesebro, Heterologous Prp molecules interfere with accumulation of protease-resistant Prp in scrapie-infected murine neuroblastoma-cells, *J. Virol.* 68 (1994) 4873–4878.
- [32] K. Kaneko, L. Zulianello, M. Scott et al., Evidence for protein X binding to a discontinuous epitope on the cellular prion protein during scrapie prion propagation, *Proc. Natl. Acad. Sci. USA* 94 (1997) 10069–10074.
- [33] L. Zulianello, K. Kaneko, M. Scott et al., Dominant-negative inhibition of prion formation diminished by deletion mutagenesis of the prion protein, *J. Virol.* 74 (2000) 4351–4360.
- [34] H.K. Edsles, V.T. Gray, R.B. Wickner, The [URE3] prion is an aggregated form of Ure2p that can be cured by overexpression of Ure2p fragments, *Proc. Natl. Acad. Sci. USA* 96 (1999) 1498–1503.
- [35] J. Chabry, B. Caughey, B. Chesebro, Specific inhibition of in vitro formation of protease-resistant prion protein by synthetic peptides, *J. Biol. Chem.* 273 (1998) 13203–13207.
- [36] C. Soto, R.J. Kascsak, G.P. Saborio et al., Reversion of prion protein conformational changes by synthetic beta-sheet breaker peptides, *Lancet* 355 (2000) 192–197.
- [37] C. Soto, E.M. Sigurdsson, L. Morelli, R.A. Kumar, E.M. Castano, B. Frangione,  $\beta$ -sheet breaker peptides inhibit fibrillogenesis in a rat brain model of amyloidosis: implications for Alzheimer's therapy, *Nat. Med.* 4 (1998) 822–826.
- [38] M.A. Findeis, G.M. Musso, C.C. Arico-Muendel et al., Modified-peptide inhibitors of amyloid  $\beta$ -peptide polymerization, *Biochemistry* 38 (1999) 6791–6800.
- [39] E. Hughes, R.M. Burke, A.J. Doig, Inhibition of toxicity in the  $\beta$ -amyloid peptide fragment  $\beta$ (25–35) using *N*-methylated derivatives — a general strategy to prevent amyloid formation, *J. Biol. Chem.* 275 (2000) 25109–25115.
- [40] D. Schenk, R. Barbour, W. Dunn et al., Immunization with amyloid- $\beta$  attenuates Alzheimer-disease-like pathology in the PDAPP mouse, *Nature* 400 (1999) 173–177.
- [41] G.C. Su, G.W. Arendash, R.N. Kalara, K.B. Bjugstad, M. Mullan, Intravascular infusions of soluble  $\beta$ -amyloid compromise the blood-brain barrier, activate CNS glial

- cells and induce peripheral hemorrhage, *Brain Res.* 818 (1999) 105–117.
- [42] A. Wegner, P. Savko, Fragmentation of actin-filaments, *Biochemistry* 21 (1982) 1909–1913.
- [43] H. Naiki, K. Hasegawa, I. Yamaguchi, H. Nakamura, F. Gejyo, K. Nakakuki, Apolipoprotein E and antioxidants have different mechanisms of inhibiting Alzheimer's  $\beta$ -amyloid fibril formation in vitro, *Biochemistry* 37 (1998) 17882–17889.
- [44] C.E. MacPhee, C.M. Dobson, Chemical dissection and reassembly of amyloid fibrils formed by a peptide fragment of transthyretin, *J. Mol. Biol.* 297 (2000) 1203–1215.
- [45] A. Yamamoto, J.J. Lucas, R. Hen, Reversal of neuropathology and motor dysfunction in a conditional model of Huntington's disease, *Cell* 101 (2000) 57–66.
- [46] J. Masel, V.A.A. Jansen, The kinetics of proteinase K digestion of linear prion polymers, *Proc. R. Soc. Lond. B Biol. Sci.* 266 (1999) 1927–1931.
- [47] B. Caughey, D.A. Kocisko, G.J. Raymond, P.T. Lansbury, Aggregates of scrapie-associated prion protein induce the cell-free conversion of protease-sensitive prion protein to the protease-resistant state, *Chem. Biol.* 2 (1995) 807–817.
- [48] G. Merlini, E. Ascari, N. Amboldi et al., Interaction of the anthracycline 4'-iodo-4'-deoxydoxorubicin with amyloid fibrils: inhibition of amyloidogenesis, *Proc. Natl. Acad. Sci. USA* 92 (1995) 2959–2963.
- [49] A. Cornish-Bowden, *Fundamentals of Enzyme Kinetics*, Portland Press, London, 1995.